EBioMedicine 65 (2021) 103242

Contents lists available at ScienceDirect

EBioMedicine

journal homepage: www.elsevier.com/locate/ebiom

Research paper

Increased co-expression of PSMA2 and GLP-1 receptor in cervical cancer models in type 2 diabetes attenuated by Exendin-4: A translational case-control study

Dandan Mao[a], Huanyi Cao[a], Mai Shi[a], Chi Chiu Wang[b], Joseph Kwong[b], Joshua Jing Xi Li[c], Yong Hou[a], Xing Ming[a], Heung Man Lee[a], Xiao Yu Tian[d], Chun Kwok Wong[e], Elaine Chow[a,f], Alice Pik Shan Kong[a,g,h], Vivian Wai Yan Lui[d], Paul Kay Sheung Chan[i], Juliana Chung Ngor Chan[a,g,h,*]

[a] Department of Medicine and Therapeutics, The Chinese University of Hong Kong, Prince of Wales Hospital, Hong Kong SAR, China
[b] Department of Obstetrics and Gynaecology, The Chinese University of Hong Kong, Prince of Wales Hospital, Hong Kong SAR, China
[c] Department of Anatomical and Cellular Pathology, The Chinese University of Hong Kong, Prince of Wales Hospital, Hong Kong SAR, China
[d] School of Biomedical Sciences, The Chinese University of Hong Kong, Hong Kong SAR, China
[e] Department of Chemical Pathology, The Chinese University of Hong Kong, Prince of Wales Hospital, Hong Kong SAR, China
[f] Phase 1 Clinical Trial Centre, The Chinese University of Hong Kong, Prince of Wales Hospital, Hong Kong SAR, China
[g] Hong Kong Institute of Diabetes and Obesity, The Chinese University of Hong Kong, Prince of Wales Hospital, Hong Kong SAR, China
[h] Li Ka Shing Institute of Health Sciences, The Chinese University of Hong Kong, Prince of Wales Hospital, Hong Kong SAR, China
[i] Department of Microbiology, The Chinese University of Hong Kong, Prince of Wales Hospital, Hong Kong SAR, China.

ARTICLE INFO

Article History:
Received 2 September 2020
Revised 26 January 2021
Accepted 28 January 2021
Available online xxx

Keywords:
Type 2 diabetes
Cancer
Exendin-4
PSMA
GLP-1R

ABSTRACT

Background: Type 2 diabetes (T2D) increases the risk of many types of cancer. Dysregulation of proteasome-related protein degradation leads to tumorigenesis, while Exendin-4, a glucagon-like peptide 1 receptor (GLP-1R) agonist, possesses anti-cancer effects.
Methods: We explored the co-expression of proteasome alpha 2 subunit (*PSMA2*) and *GLP-1R* in the Cancer Genome Atlas (TCGA) database and human cervical cancer specimens, supplemented by *in vivo* and *in vitro* studies using multiple cervical cancer cell lines.
Findings: PSMA2 expression was increased in 12 cancer types in TCGA database and cervical cancer specimens from patients with T2D (T2D vs non-T2D: 3.22 (95% confidence interval CI: 1.38, 5.05) vs 1.00 (0.66, 1.34) fold change, $P = 0.01$). *psma2*-shRNA decreased cell proliferation *in vitro*, and tumour volume and Ki67 expression *in vivo.* Exendin-4 decreased *psma2* expression, tumour volume and Ki67 expression *in vivo*. There was no change in *GLP-1R* expression in 12 cancer types in TCGA database. However, *GLP-1R* expression (T2D vs non-T2D: 5.49 (3.0, 8.1) vs 1.00 (0.5, 1.5) fold change, $P < 0.001$) was increased and positively correlated with *PSMA2* expression in T2D-related ($r = 0.68$) but not in non-T2D-related cervical cancer specimens. This correlation was corroborated by *in vitro* experiments where silencing *glp-1r* decreased *psma2* expression. Exendin-4 attenuated phospho-p65 and -IκB expression in the NF-κB pathway.
Interpretation: *PSMA2* and *GLP-1R* expression in T2D-related cervical cancer specimens was increased and positively correlated, suggesting hyperglycaemia might promote cancer growth by increasing *PSMA2* expression which could be attenuated by Exendin-4.
Funding: This project was supported by Postdoctoral Fellowship Scheme, Direct Grant, Diabetes Research and Education Fund from the Chinese University of Hong Kong (CUHK)
© 2021 The Authors. Published by Elsevier B.V. This is an open access article under the CC BY-NC-ND license (http://creativecommons.org/licenses/by-nc-nd/4.0/)

1. Introduction

Diabetes increases the risk of many cancer types and cancer-related death, particularly in liver, pancreas, colorectal cancer, and lung cancer [1]. In patients with type 2 diabetes (T2D), a 1% increase in HbA_{1C} is associated with 1.18-fold increased risk of cancer [2,3].

* Corresponding author at: Department of Medicine and Therapeutics, The Chinese University of Hong Kong, Prince of Wales Hospital, 30-32 Ngan Shing St, Shatin, N.T., Hong Kong SAR, China.
E-mail address: jchan@cuhk.edu.hk (J.C.N. Chan).

https://doi.org/10.1016/j.ebiom.2021.103242
2352-3964/© 2021 The Authors. Published by Elsevier B.V. This is an open access article under the CC BY-NC-ND license (http://creativecommons.org/licenses/by-nc-nd/4.0/)

Research in context

Evidence before this study

Diabetes increases the risk of cancer and cancer-related death. Inflammation is common in cancer and diabetes, especially for virus infection-induced cancer, e.g., human papillomavirus (HPV)-16 and -18 related cervical cancer. The ubiquitin-proteasome system is responsible for protein homeostasis, which is disrupted in carcinogenesis. Exendin-4 has been shown to attenuate cancer growth in prostate, pancreatic, and breast cancer. We previously reported the attenuating effect of Exendin-4 on tumour growth in *db/db* mice induced by mouse epithelial cervical cancer cells (CUP-1, The Chinese University of human Papilloma virus-1).

Added value of this study

We demonstrated the proto-oncogenic role of PSMA2 in cervical cancer specimens from patients with T2D with corroborative evidence from cellular and animal models. Importantly, we discovered the increased co-expression of GLP-1R and PSMA2 in human and experimental models of cervical cancer, promoted by hyperglycemia but attenuated by Exendin-4.

Implications of all of the available evidence

Since proteasome inhibitors and GLP-1 mimetics are in clinical use, our data have strong translational potential. Given the increased co-expression of *GLP-1R* and *PSMA2* in cervical cancer and the proto-oncogenic role of PSMA2, GLP-1R agonist might have the potential to treat cancer especially in patients with T2D.

Sexual activity-related cancer, including cervical, oropharyngeal, and anal cancers due to infection of human papillomavirus (HPV)-16 and -18 [4], are not uncommon in T2D. Inflammation, often associated with low-grade chronic infection, plays an important role in carcinogenesis. As such, the co-existence of diabetes and virus infection may create an inflammatory microenvironment to promote cancer cell growth [2,5]. Moreover, T2D is associated with poor survival in patients with cervical cancer, making T2D an important prognostic factor for cervical cancer [6].

Genetic mutations, chemical irritation, irradiation, toxins, bacteria, and virus infections are amongst the common causes of tumorigenesis [7,8]. Cancer is characterized by perturbation of cell growth and proliferation. The uncontrolled cell proliferation is supported by high protein turnover in cancer cells. The ubiquitin-proteasome system is essential for the maintenance of cellular protein homeostasis, i.e. the balance between normal protein synthesis and protein degradation [9]. An abnormal protein is first tagged by ubiquitin for its transfer to the cylinder-like structure of the proteasome complex with alpha and beta subunits for degradation into small peptides [10]. Increased proteasome expression or activity may contribute to carcinogenesis by promoting robust protein turnover [11]. Inhibition of the proteasome results in cell-cycle arrest and apoptosis, and is a target for anticancer therapy [12]. Recently, a proteasome gene, namely *PSMA2*, has been identified to promote breast cancer cell growth, indicative of its potential proto-oncogenic role in cancer [13]. A single nucleotide polymorphism (SNPs) c.328C>G, contributing to missense protein-coding in *PSMA2,* has been implicated in human breast and colorectal cancer [14,15].

In clinical practice, proteasome inhibitors, such as bortezomib and carfilzomib, are antitumor drugs approved for the treatment of multiple myeloma and lymphoma [16]. The inhibitor-κB (IκB)-nuclear factor-κB (NF-κB) pathway promotes inflammation which can lead to abnormal cell growth. Increased expression of proteasome can degrade IκB and release NF-κB with nuclear translocation to activate transcription of the inflammatory cytokines and cell signals. By blocking IκB degradation, proteasome inhibitors can prevent nuclear translocation of NF-κB and inhibit tumour growth [7].

GLP-1 is an incretin hormone released from the L cells in the lower intestine. It can augment insulin release during meal-time and suppress glucagon production [17]. Glucagon-like peptide 1 mimetics include GLP-1 receptor agonist, such as Exendin-4 which binds with GLP-1R, and dipeptidyl peptidase 4 [DPP-4] inhibitor which inhibits the degradation of GLP-1. These new classes of blood glucose-lowering drugs carry a low risk of hypoglycaemia with weight-neutral or weight-reducing effects [18,19].

There are emerging reports on the anti-cancer effects of GLP-1 mimetics although the mechanisms require further elucidation. Exendin-4 has been shown to attenuate the proliferation of human prostate cancer cells through inhibition of extracellular signal-regulated kinase (ERK)-mitogen-activated protein kinase (MAPK) [20]. In patients with prostate cancer, Exendin-4 enhanced the responsiveness to chemotherapy and reduced cancer growth by activating the phosphatidylinositol-3-kinase (PI3K)/Akt/mTOR (the mammalian target of rapamycin) pathways [21]. In human pancreatic and breast cancer cell lines, GLP-1R agonist, liraglutide, attenuated cancer growth by inhibiting cellular proliferation and inducing apoptosis through inhibition of the NF-κB pathway [22,23]. In a meta-analysis of randomized controlled trials (RCTs) involving 63,594 patients with T2D, subgroup analyses indicated that treatment with albiglutide, a GLP-1 agonist, was associated with 24% (95% confidence interval (CI) 0.60-0.97) reduction of all-site cancer compared with the placebo group. However, the number of cancer cases was only 91 in the treatment group and 119 in the placebo group [24].

In experimental studies, GLP-1 has been shown to exert anti-inflammatory effects in multiple organs, including the heart, brain, kidney, liver, pancreas, skin, and testis [25]. This effect was in part mediated by suppressing the immune system such as macrophages, dendritic cells, and mast cells with reduced release of pro-inflammatory cytokines (e.g., interleukin (IL)-1β, IL-6, IL-12), nitric oxide (NO), and tumour necrosis factor (TNF)-α [26]. In this light, our group has reported the *ex vivo* inhibitory effects of Exendin-4 on the release of cytokines from peripheral blood mononuclear cells extracted from patients with T2D [27].

Using the Hong Kong Diabetes Register established since 1995, our group was amongst the first to report the high incidence of cancer in Chinese patients with T2D, which was closely associated with glycaemia [28,29]. These epidemiological studies have motivated our group to develop the CUP-1 epithelial cancer cell line to explore the mechanisms of this diabetes-cancer link. The CUP-1 is an immortal mouse epithelial cancer cell line generated from the kidney of baby C57BL/6J mice with the insertion of the HPV-16 E7 oncogene [30]. We established a diabetes/cancer model by subcutaneous inoculation of CUP-1 cancer cells in the diabetic *db/db* mice, followed by tumour growth to a maximum volume by day 14. Compared with vehicle, Exendin-4 attenuated the tumour growth [31] although the underlying mechanism remains unknown.

Both cancer and T2D are characterized by excessive protein turnover. Given the importance of proteasome in protein homeostasis, we interrogated TCGA database and noted increased expression of *PSMA2* in 12 cancer types based on human samples, including cervical cancer. Supported by these clinical findings, we explored the effect of high glucose on *PSMA2* expression in cervical cancer including human, *in vivo*, and *in vitro* systems. To further explore the anti-tumour effects of Exendin-4 reported in our previous experiment [31], we examined the expression of *GLP-1R* and the effect of Exendin-4 on *psma2* expression and tumour growth and associated changes in the NF-κB pathway using cellular, animal and human samples.

Firstly, we hypothesize that PSMA2 expression was increased in cervical cancer from patients with T2D. Secondly, PSMA2-O/E and -shRNA increased and decreased cell proliferation under high glucose condition and tumour volume in *db/db* mice, respectively. Thirdly, high glucose increased GLP-1R expression *in vitro* and Exendin-4 reduced PSMA2 expression, decreased cell proliferation, and attenuated tumour volume. Lastly, GLP-1R expression was increased in cervical cancer specimens from patients with T2D.

We used complementary human specimens, *in vivo*, and *in vitro* models to test these hypotheses. We first examined PSMA2 expression in cervical cancer specimens from patients with T2D, followed by human and mouse cervical cancer cell lines. Secondly, we generated stable cell lines with *psma2*-O/E or -shRNA transfection in CUP-1 cells to explore the role of *psma2* in cell proliferation and tumour growth. Thirdly, we examined the effect of Exendin-4 on *psma2* expression, cell proliferation, and tumour growth. Fourthly, we examined GLP-1R expression and its correlation with PSMA2 expression in cervical cancer specimen from patients with T2D, followed by confirmation from cervical cancer cell lines. Lastly, we explored the effects of high glucose and Exendin-4 on the NF-κB pathway, including phospho-p65 and phospho-IκB levels.

2. Methods

2.1. Pan-cancer expression of PSMA2 and GLP-1R

TCGA database has comprehensive cancer genomic profiles, including transcriptomic data of over 30 human tumours [32]. Our bioinformaticist (MS) extracted publicly available mRNA expression profiles of PSMA2 and GLP-1R generated from RNA-sequencing experiments, and analysed their differences using Gene Expression Profiling Interactive Analysis 2 [33]. We examined 13 types of cancer including invasive breast carcinoma (BRCA), cervical squamous cell carcinoma and endocervical adenocarcinoma (CESC), cholangiocarcinoma (CHOL), colon adenocarcinoma (COAD), lymphoid neoplasm diffuse large B-cell lymphoma (DLBC), oesophageal carcinoma (ESCA), head and neck squamous cell carcinoma (HNSC), liver hepatocellular carcinoma (LIHC), lung squamous cell carcinoma (LUSC), pancreatic adenocarcinoma (PAAD), rectum adenocarcinoma (READ), stomach adenocarcinoma (STAD), and thymoma (THYM). For each type of cancer, the gene expression was matched with that in normal samples in the Genotype-Tissue Expression (GTEx) database [34].

2.2. Cell lines and treatment

We used cancer cell lines including human breast cancer cell line MCF-7 (RRID: CVCL_0031), and non-cancerous cell lines including mouse fibroblastic cell line L929 (RRID: CVCL_0462) and human embryonic kidney cell line 293 (RRID: CVCL_0045) to conduct a series of experiments. These cell lines were cultured in DMEM medium (Cat. 11885076, Invitrogen, USA) with 10% FBS (Cat. 26140079, fetal bovine serum) (Gibco, USA), and 1% Antibiotic-Antimycotic (Amphotericin B, Penicillin, Streptomycin) (Cat. 15240112, Gibco, USA). We included three human cervical cancer cell lines SiHa (RRID: CVCL_0032), HeLa (RRID: CVCL_0030), and C33A (RRID: CVCL_1094), which were cultured in MEM medium (Cat. 12571071, Invitrogen, USA) with 10% FBS, and 1% Antibiotic-Antimycotic. These cell lines have been validated by Department of Anatomical and Cellular Pathology core laboratory at the CUHK using DNA fingerprinting.

Our group established CUP-1 by incorporating HPV-16 E7 and activated EJ-ras oncogene into baby mouse kidney epithelial cells from C57BL/KSJ mice, which shares the same genetic background of *db/db* mice. We immortalized the cell line with stable expression of HPV-16 E7 oncogene, which was inoculated in *db/db* mice for tumour development [30,31]. CUP-1 cells were cultured in DMEM medium (Cat. 11885076, Invitrogen, USA) with 10% FBS, and 1% Antibiotic-Antimycotic.

The above cell lines underwent overnight serum starvation in medium with normal glucose and low FBS (1%). The culture medium was replaced with fresh medium with low (2.8mmol/L), normal (5.5 mmol/L) or high glucose (25 mmol/L) for 48h for molecular analysis. CUP-1 cells were treated with Exendin-4 (Cat. E7144, Sigma-Aldrich, US) at concentrations of 0, 5, 20, and 50 nmol/L for 6, 24, and 48 h. Cells for *in vitro* studies were passaged from one relevant cell lines in the same condition with highly homogenous phenotypes. All *in vitro* experiments were repeated at least twice with at least 3 samples in each experiment, hence results of 6 samples were analysed and presented.

2.3. Human tissue

A case-control study were conducted to compare the RNA and protein differences in PSMA2 and GLP-1R expression in cervical cancer specimens from patients with or without T2D. All specimens were obtained during radical hysterectomy performed at the Prince of Wales Hospital (PWH), the teaching hospital of the CUHK, between January 2016 and July 2019. We retrieved frozen tissue and histological samples of age-matched patients with or without T2D. Frozen samples were used for RNA expression analysis and cut into 3-mm sections for microdissection using a fine surgical blade to isolate tumour-specific cells under an inverted microscope.

The medical records of these patients were reviewed using the territory-wide electronic medical system shared by all publicly-funded hospitals and clinics. Diabetes was defined based on physician-diagnosed T2D and/or prescription of glucose-lowering drugs and/or abnormal laboratory values as defined by the American Diabetes Association guidelines: HbA1c $\geq$ 6.5%, or fasting plasma glucose $\geq$ 7.0 mmol/L, or 2-h plasma glucose $\geq$ 11.1 mmol/L during a 75 g oral glucose tolerance test (OGTT), or random plasma glucose $\geq$ 11.1 mmol/L with typical symptoms of hyperglycemia or hyperglycaemic crisis.

2.4. Animal experiments, tumour induction, and oral glucose tolerance test

10-week old male *db/db* mice (Jackson Stock #000642, BKS.Cg-Dock7^{m}+/+Lepr^{db} /J) were obtained from the CUHK Laboratory Animal Services Centre and transferred to the Animal House of the Li Ka Shing Institute of Health Sciences (LKS) based at the PWH. All mice were housed in a temperature-controlled room (22 °C) on a 12-h light-dark cycle with free access to food and water at the PWH.

To examine the cancer-promoting effect of PSMA2 and anti-cancer effect of Exendin-4, we inoculated *db/db* mice with the same number (2×10^7) of CUP-1 cells, *psma*2-shRNA transfected CUP-1 cells, or *psma*2-vector transfected CUP-1 cells subcutaneously underneath the nape of the neck (scruff). After inoculation (Day 0), the mice were assigned to receive either a daily intraperitoneal injection of Exendin-4 (30 nM/kg body weight) [31] or PBS for 13 days with 7−10 mice in each group.

On day 3, tumour developed at the scruff of the mice, and the size was measured by calliper (Mitutoyo, Taiwan) twice weekly during the treatment period. Tumour volumes were calculated using the equation $V = (a \times b^2) \times 0.5236$, where "a" was the larger dimension and "b" the perpendicular diameter [35]. Bodyweight, food consumption, and random blood glucose were also measured twice weekly during the treatment period. None of the mice developed a tumour larger than 2×2 cm^2 to meet the exclusion criteria.

On day 14, an oral glucose tolerance test (OGTT) was performed after overnight fasting for 15 h to examine the anti-diabetic effects of Exendin-4. For OGTT, the mice were gavaged with 20% glucose (1 g/kg) after blood collection at baseline (0 min). All blood samples were

collected from the tail vein at 0, 15, 30, 60, and 120 min for glucose measurements, followed by tumour collection for histological analysis. Mice were sacrificed by inhalation of carbon dioxide provided by the LKS Animal House based at the PWH.

2.5. Plasmid, shRNA, and siRNA transfection

For *psma2* overexpression plasmid construction, mouse cDNA encoding *psma2* was amplified using the following primers: forward (F) 5'- GAGCGCGGTTACAGCTTCT-3', reverse (R) 5'- GCAGCTTTAATCCCCACTGAC-3'. The amplified fragment was sub-cloned into pcDNA3.1+ vector between BamH1(5') and XhoI (3') restriction sites and confirmed by sequencing analysis. The above plasmid DNA fragment was sent to Hanbio (China) for lentiviral expression and packaging.

For *psma2* knockdown, shRNA lentivirus particles were purchased from Sigma (Cat. SH0731, USA) and used according to the manufacturer's instructions. Lentivirus overexpression (20 μL of 1×10^6 viral titre) or downregulation (200 μL of 1×10^5 viral titre) particles were added to the wells for transfection. After 12 h, the medium with lentivirus particles was replaced with fresh medium for incubation for 48h, followed by puromycin selection for at least 14 days. The surviving cells were examined for *psma2* expression by RT-PCR and used as cell lines with stable *psma2* overexpression or downregulation for molecular and animal studies.

For GLP-1R knockdown, siRNA was purchased from Invitrogen (Cat. 4390771, USA) and used according to the manufacturer's instructions. 15 pmol siRNA particles together with lipofectamine 2000 (Cat. 11668027, Invitrogen, USA) were added to the wells for transfection. After 12 h, the medium was replaced with fresh medium for incubation for 48 h. Western blotting (WB) was performed to validate GLP-1R downregulation.

2.6. MTT and cell proliferation assay

We seeded 1000−2000 cells into each well of 96-well plate for overnight incubation. After treatment based on different experimental design, we added 10 μL MTT Reagent (Sigma-Aldrich, USA) into the cell medium for incubation for 4 h until a purple precipitate was visible. The cell medium was replaced with 100 μL DMSO for 2 h-incubation in the dark, followed by an absorbance record at 570 nm.

3000 cells of each cell line were seeded in 96-well cell culture plates for overnight incubation. After treatment based on different experimental design, cell proliferation was analysed daily up to 72 h by cell counting using a haemocytometer.

2.7. Histological staining

We used human cervical cancer histological samples from Department of Anatomical and Cellular Pathology CUHK for PSMA2 and GLP-1R immunofluorescence (IF) staining. Mice tumour was collected after treatment and fixed in 4% (v/v) paraformaldehyde overnight and embedded in paraffin. Sections were cut to 4 μm thickness for IF staining of Ki67 and PSMA2.

For IF staining, after rehydration, slides were placed in 0.5% (v/v) triton X for 20 min for permeabilization, followed by 0.01 mol/L sodium citrate buffer (pH 6.0) and heated at ~100 °C for 10 min for antigen retrieval. After blocking nonspecific antigens, rabbit anti-Ki67, PSMA2, or GLP-1R antibody was applied to the sections overnight at 4 °C. The sections were then washed in PBST three times and incubated with fluorescence-conjugated secondary antibodies, Alexa Fluor® goat anti-rabbit 555 at room temperature (RT) for 1 h, followed by counterstaining of the nucleus with DAPI. The images were captured using the Leica Qwin image analysis software (Leica, Germany). Table S1 lists the antibodies used in these experiments. Images of at least 10 vision fields were captured in each slide and positive signals were quantified using Image J.

2.8. Real-time PCR and immunoblotting

We used Trizol (Invitrogen, USA) to extract total RNA in all cell models, followed by reverse transcription to cDNA (Takara, Japan). cDNA was applied to SYBR-Green Kit (Promega, USA) and then Applied Biosystems 7900HT for quantitative RT-PCR analysis. Mouse primers are shown in table S1.

Total proteins from cells were extracted using ice-cold cell lysis buffer (Cat. #9803, Cell Signalling Technology, USA) supplemented with protease inhibitor (Roche, Switzerland) and Na_3VO_4 and then adjusted to the same concentration by loading buffer and denatured. After gel electrophoresis, transfer and blocking, membranes were incubated in the primary antibodies at 4 °C overnight. The primary antibodies included PSMA2, GLP-1R, phospho-P65, P65, phospho-IκB, IκB, and GAPDH. HRP-linked anti-rabbit and anti-mouse IgG were used as secondary antibodies. Protein bands were developed by Immobilon Western Chemiluminescent HRP Substrate (Millipore, Billerica, MA, USA). Table S1 lists the antibodies used in these experiments.

2.9. Statistical analysis

In TCGA data analysis, for each type of cancer, we used ANOVA to compare expression profiles between cancerous and normal samples. Statistical significance was defined as an absolute log2 fold change $>$ 0.5 and a p-value $<$ 0.001.

In animal experiments, we calculated the sample size to be 7 in each group (28 in total) based on the mean and standard deviation (SD) (mean±SD) of tumour volume in the Exendin-4 group (500± 110 mm^2) and control group (700±120 mm^2) in a pilot study (n = 3 in each group), to achieve 90% power with an alpha (p) value less than 0.05. Mice were randomly assigned to treatment or control group. Treatment and measurements were performed at the same time daily and in a random order to minimise potential confounders. The conduct of experiment, tumour size measurements, and data analysis were performed by different investigators blinded to the treatment group. Mice were excluded if the tumour volume exceeded 2×2 cm^2. All data are presented as mean±SD (95% CI) with individual data point shown in histograms. We plotted the data to confirm their normal distribution. We used Student's t-test and two-way ANOVA with Tukey's post hoc test, as appropriate, to examine between-group differences using Prism (GraphPad Prism 7, San Diego, CA, USA) with significance defined as $p < 0.05$.

In the analysis of human cervical cancer specimens, we included patients who underwent hysterectomy for cervical cancer at the PWH in 2016−2019, who consented to donate their cancer specimens for research. We excluded those with immunodeficiency or active substance abuse and identified patients who met inclusion criteria for T2D and selected control subjects matched by age. We performed a pilot study with 3 samples in each group and calculated a sample size of 9 in each group was required based on the mean±SD of PSMA2 RNA expression in the non-T2D group (1±1.4) and T2D group (3 ± 1.5, fold change) to achieve a power of 0.8 with an alpha (p) value less than 0.05. The experiments and data analysis were conducted with the analyst blinded to the group assignment. We compared PSMA2 and GLP-1R expression between the T2D and non-T2D group and performed correlation analysis in each group. A p-value $<$ 0.05 (2-tailed) was considered as statistically significant.

2.10. Ethics

The human study protocol was approved by the Joint CUHK-New Territories East Cluster Clinical Research Ethics Committees (CREC

Ref. No.: 2018.457). All patients gave written informed consent for research and publication purposes. The animal experimental protocol was approved by the Animal Experimentation Ethics Committee of CUHK (AEEC Ref. No.: 17-089-MIS). All animal procedures were compliant with guidelines on animal use.

2.11. Role of the funding source

The funders had no role in experimental design, data collection, data analyses, interpretation, or manuscript writing. We were not paid to write this article by any company or agency. The corresponding author had full access to all data in this study.

2.12. Results

1 Increased PSMA2 expression in 12 human cancer types and cervical cancer specimens from patients with T2D, further confirmed in multiple cervical cancer cell lines.

We identified tumour-specific overexpression of *PSMA2* in 12 types of cancer from TCGA database, compared with respective normal tissues from the GTEX database. These included breast, cervical, cholangial, colorectal, lymphoid, oesophageal, head and neck, liver, lung, pancreatic, stomach, and thymus cancer (Fig. 2a). Based on the statistically significant increase in *PSMA2* expression in cervical cancer, and the emerging role of *PSMA2* in both cancer and diabetes [13,14,36], we examined *PSMA2* expression in cervical cancer specimens from patients with or without T2D, multiple human and mouse cervical cancer cell lines and non-cancerous cell lines.

Fig. 1 lists the flowchart of participant selection for analysis of PSMA2 expression in cervical cancer specimens. Table 2 lists the clinical characteristics of the selected participants in this study. We retrieved these subjects' specimens for IF staining and RT-PCR analysis for PSMA2 expression. In Fig. 2b and c, patients with T2D had higher PSMA2 protein expression than those without T2D (T2D: 0.59%, 95% CI: 0.47−0.72; Non-T2D: 0.36%, 95% CI: 0.25−0.46; P = 0.004, t-test) (n = 9 in each group). In Fig. 2d, RT-PCR analysis revealed a 3-fold increase in *PSMA2* expression in patients with T2D (T2D: 3.22 (fold change), 95% CI: 1.38−5.05; Non-T2D: 1.00, 95% CI: 0.66−1.34; P = 0.01, t-test).

To test the hypothesis of whether high glucose condition would alter the expression of this potential proto-oncogene, we determined the *PSMA2* expression in multiple epithelial cervical cancer cell lines. High glucose (25 mmol/L) increased *PSMA2* expression in SiHa (P = 0.04, t-test), HeLa (P = 0.04, t-test), and C33A cells (P = 0.04, t-test), but not in non-cancerous mouse fibroblast and human embryonic kidney cells (Fig. 2e). In CUP-1 cells, exposure to high glucose also upregulated *psma2* expression in a glucose-dose-dependent manner (normal glucose (NG) vs low glucose (LG): ~1.5 folds, P = 0.008, t-test; HG vs NG: ~1.5 folds, P = 0.04, t-test) (Fig. 2f).

2 *Psma2*-O/E and -shRNA increased and decreased cell proliferation and tumour volume respectively under high glucose environment

We treated CUP-1 cells with *psma2*-O/E or -shRNA under normal or high glucose condition followed by cell viability and proliferation assay. High glucose promoted cell proliferation in CUP-1 cells (P = 0.001, t-test). Enforced *psma2*-O/E transfection also promoted CUP-1 cell proliferation under normal (P = 0.002, *t-test*) and high glucose conditions (P = 0.005, *t-test*) (Fig. 3a and b). Consistent with the above results, *psma2*-shRNA reduced cell viability and proliferation in normal and in high glucose conditions *in vitro* (Fig. 3c and d). The RNA and protein expression of PSMA2 in the above conditions was confirmed (Fig. 3e-h).

To determine the role of *psma2* in the hyperglycaemic background *in vivo*, we inoculated CUP-1 cells, or *psma2*-shRNA transfected CUP-1 cells into *db/db* mice to induce tumour development. Mice inoculated with *psma2*-shRNA-CUP-1 cells had smaller tumour volume, compared with vector control group (P = 0.002, ANOVA test) (Fig. 3i and j). Tumour with *psma2*-shRNA-CUP-1 cells had decreased Ki67 expression, indicative of reduced tumour proliferation *in vivo* (PSMA2-shRNA vehicle: 0.26%, 95% CI: 0.09−0.42; vector control: 0.46%, 95% CI: 0.32−0.60; P = 0.028, *t-test*) (Fig. 3k and l). Downregulation of *psma2* did not alter blood glucose level *in vivo*, suggesting that the anti-cancer effect was not glucose-mediated (SFig. 2a−c).

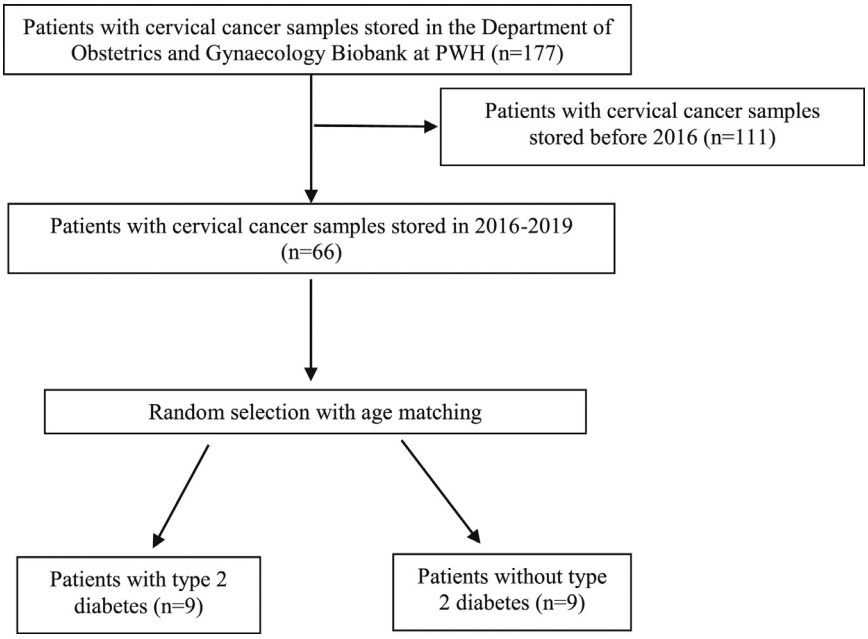

Fig. 1. Flowchart of participant selection for analysis of cervical cancer.

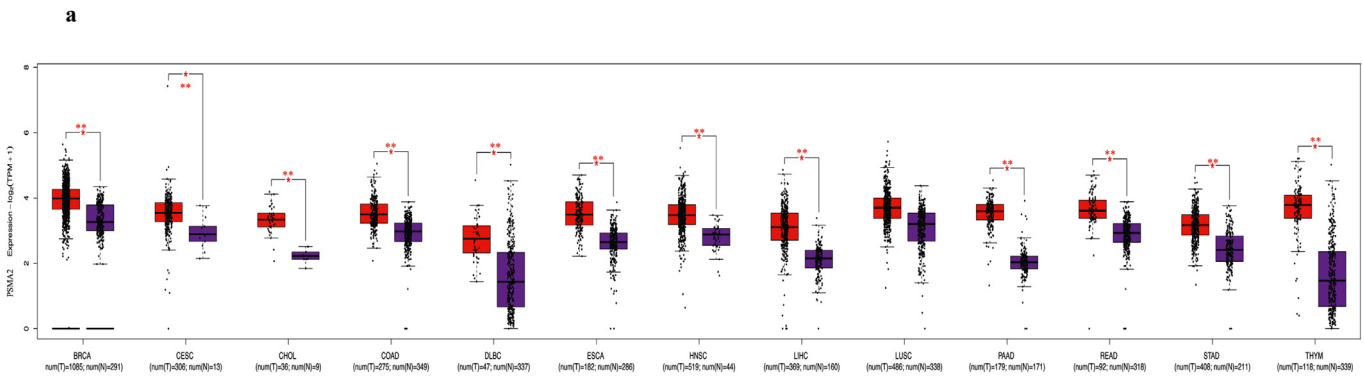

BRCA: Breast invasive carcinoma, CESC: Cervical squamous cell carcinoma and endocervical adenocarcinoma, CHOL: Cholangial carcinoma, COAD: Colon adenocarcinoma, DLBC: Lymphoid Neoplasm Diffuse Large B-cell Lymphoma, ESCA: Esophageal carcinoma, HNSC: Head and Neck squamous cell carcinoma, LIHC: Liver hepatocellular carcinoma LUSC: Lung squamous cell carcinoma, PAAD: Pancreatic adenocarcinoma, READ: Rectum adenocarcinoma, STAD: Stomach adenocarcinoma, THYM: Thymoma

Red: cancer, purple: control ***P<0.001

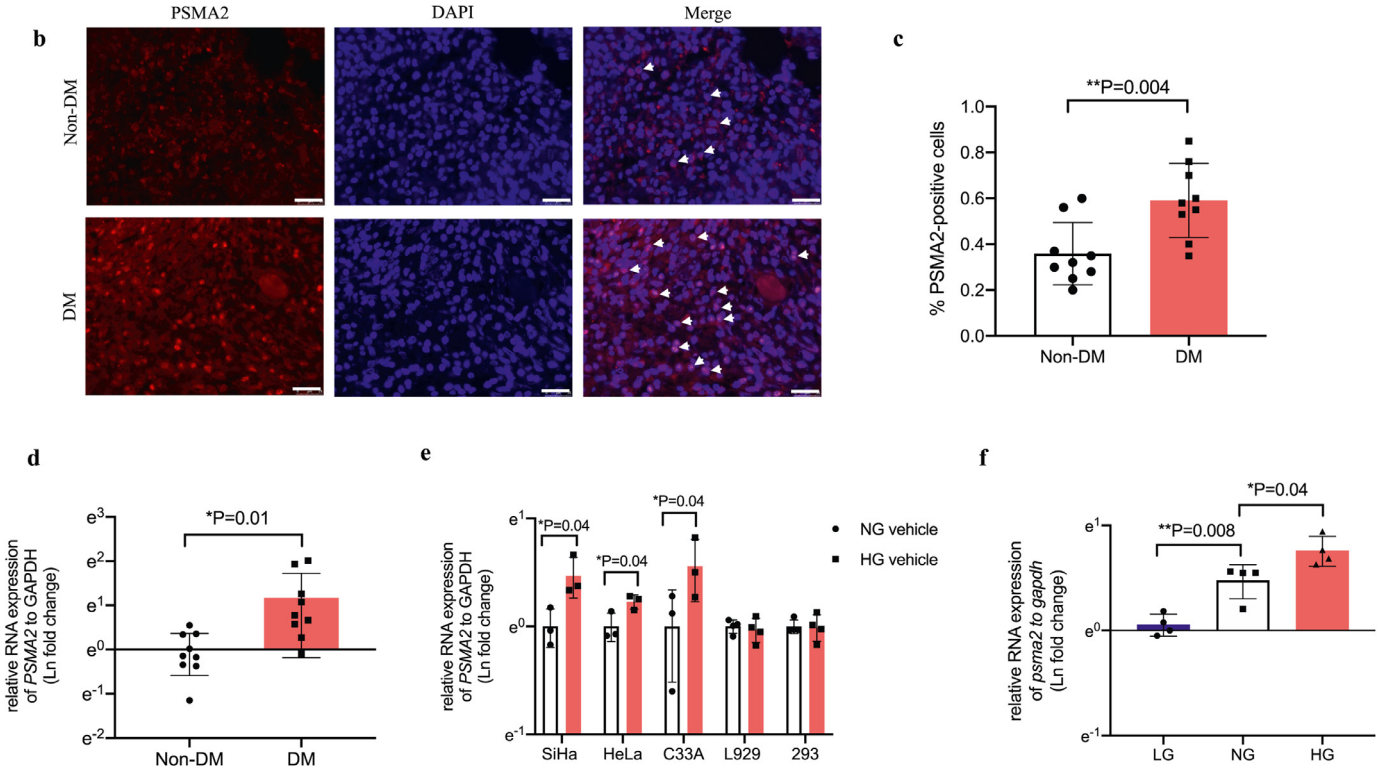

Fig. 2. Increased PSMA2 expression in 12 human cancer types and cervical cancer specimens from patients with T2D, further confirmed in multiple cervical cancer cell lines. *PSMA2* expression was examined in 13 types of cancer in TCGA database (a). Representative images of *PSMA2* expression in cervical cancer specimens from patients with and without T2D (b) (red: PSMA2, blue: DAPI, magnification: × 400. The white scale bar represents 25 μm). Relative quantification of PSMA2-positive cells (c). RNA expression of *PSMA2* was measured in cervical cancer specimens from patients with and without T2D (d) human cervical cancer cell lines SiHa, HeLa, and C33A, and non-cancerous mouse fibroblast cells (L929) as well as human embryonic kidney cells (293) (e), and CUP-1 cells (f) in low glucose, or normal glucose, or high glucose medium by RT-PCR. Data are presented as mean±SD with individual data points in histograms. * $p < 0.05$, ** $p < 0.01$, *** $p < 0.001$. (For interpretation of the references to color in this figure legend, reader can refer to the web version of this article.)

3 Exendin-4 reduced PSMA2 expression, cell proliferation, and tumour volume *in vitro* and *in vivo*

We treated human and mouse (CUP-1) cervical cancer cell lines with Exendin-4 to examine *PSMA2* expression. We treated *psma2*-O/E-CUP-1 cells and *psma2*-shRNA-CUP-1 cells with Exendin-4 under normal or high glucose condition for cell viability and proliferation assay. Under high glucose condition, Exendin-4 (50 nmol/L) decreased *PSMA2* expression in CUP-1 cells by 3-fold ($P = 0.01$, *t-test*, Fig. 4a) and in SiHa ($P = 0.01$, *t-test*), HeLa ($P < 0.001$, *t-test*), and C33A ($P = 0.04$, *t-test*) cells (Fig. 4h). Exendin-4 did not alter *psma2* expression and cell proliferation in *psma2*-shRNA-CUP-1 cells (Fig. 4b-d). In *psma2*-O/E-CUP-1 cells, Exendin-4 reduced *psma2* expression by 60% ($P = 0.003$, *t-test*) and cell viability and proliferation ($P < 0.001$, ANOVA) under high glucose condition (Fig. 4e–g).

We inoculated CUP-1 cells into *db/db* mice to induce tumour development with or without Exendin-4 treatment. Consistent with the above *in vitro* findings, Exendin-4 treatment reduced the tumour volume ($P < 0.001$, ANOVA test), starting from day 7 (Exendin-4 vs vehicle control: 513.6 (95% CI: 408.4–618.7) vs 749.9 (95% CI:

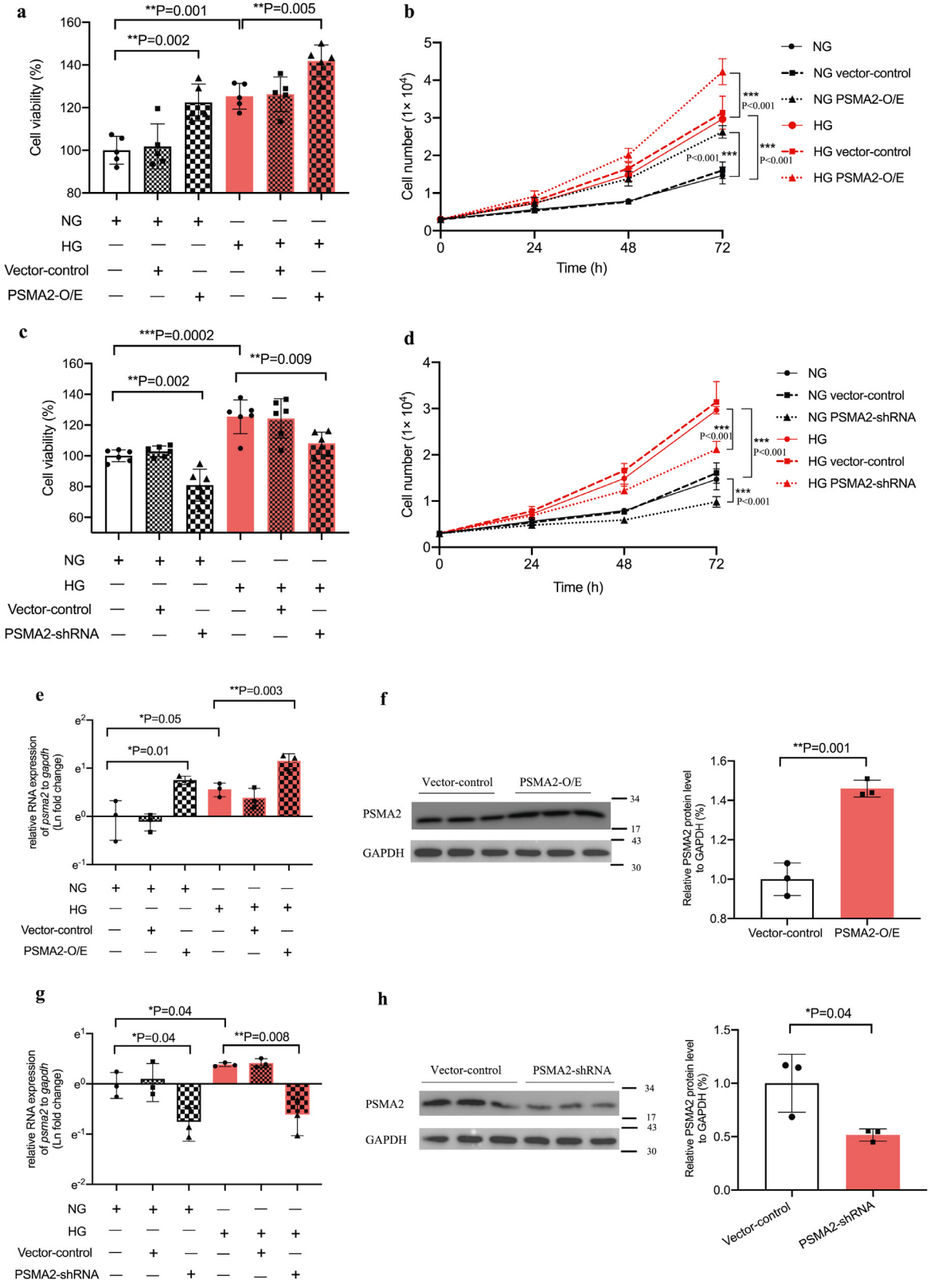

Fig. 3. *Psma2*-O/E and -shRNA increased and decreased cell proliferation and tumour volume respectively under high glucose environment Cell viability (a) and proliferation (b) were measured in CUP-1 cells with and without *psma2*-O/E in normal or high glucose medium by MTT and cell counting. The upregulation of the RNA and protein expression of *psma2* was confirmed after enforced overexpression by RT-PCR and WB (e, f). Cell viability (c) and proliferation (d) were measured in CUP-1 cells with and without *psma2*-shRNA in normal or high glucose medium by MTT and WB. Downregulation of the RNA expression of *psma2* was confirmed after *psma2*-shRNA transfection by RT-PCR and WB (g, h). (e-f) Tumour volume was measured twice weekly after inoculation of CUP-1 cells with *psma2*-shRNA or vector into *db/db* mice ($N = 7$ in each group) (i, j). Cell proliferation marker Ki67 (k, l) was measured in the tumour of the above diabetes/cancer mice (red: Ki67, blue: DAPI, magnification: × 200. The white scale bar represents 50 μm). Data are presented as mean±SD with individual data points in histograms. * $p < 0.05$, ** $p < 0.01$, *** $p < 0.001$. (For interpretation of the references to color in this figure legend, reader can refer to the web version of this article.)

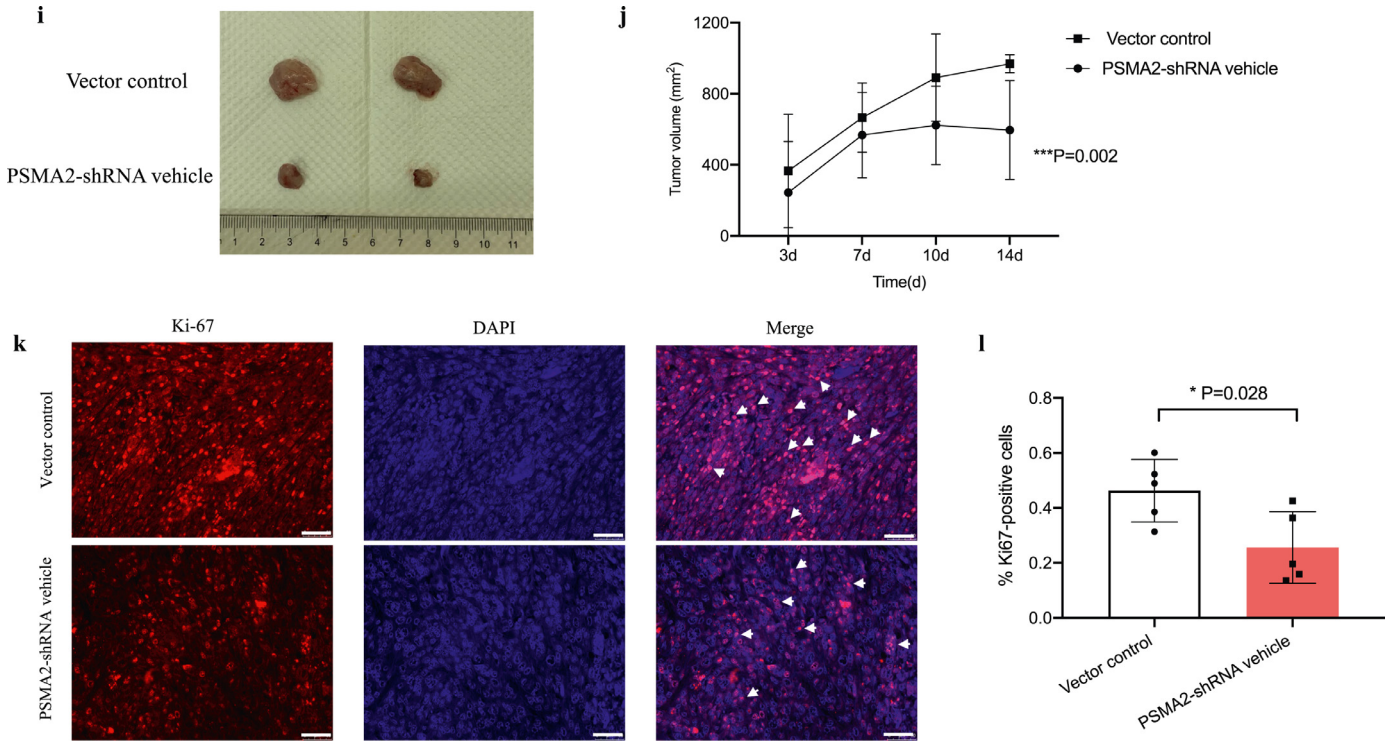

Fig. 3. Continued.

639.4–860.4) mm^2, P = 0.003, *t-test*) (Fig. 4i and j). Exendin-4 decreased Ki67 (Exendin-4: 0.27%, 95% CI: 0.07–0.47; vehicle control: 0.47%, 95% CI: 0.35–0.59; P = 0.04, *t-test*) (Fig. 4k and l) and PSMA2 expression (Exendin-4: 0.39%, 95% CI: 0.23–0.55; vehicle control: 0.61%, 95% CI: 0.44–0.78; P = 0.03, *t-test*) in tumours, compared with the vehicle-treated group (Fig. 4m and n).

4 In human cervical cancer specimen, GLP-1R expression was increased and positively correlated with *PSMA2* expression in patients with T2D, supplemented by experimental evidence in multiple cervical cancer systems.

To understand why Exendin-4 exerted the aforementioned effects, we first examined the RNA expression of *GLP-1R* in 13 types of cancer from TCGA database. There was no expression difference between tumour tissues and respective normal tissues, although diabetes status in these patients was unknown (Fig. 5a). We then analysed the protein and RNA expression of GLP-1R in human cervical cancer specimens and multiple cervical cancer cell lines. We found a 2-fold increase in GLP-1R protein expression (T2D: 0.39%, 95% CI: 0.30–0.48; Non-T2D: 0.21%, 95% CI: 0.13–0.30; P = 0.004, *t-test*) (Fig. 5b and c) and a 5-fold increase in *GLP-1R* RNA expression in cervical cancer specimens from patients with T2D, compared with those without T2D (T2D: 5.49 (fold change), 95% CI: 3.00–7.98; Non-T2D: 1.00, 95% CI: 0.5–1.5; P = 0.003, *t-test*) (Fig. 5d). We performed correlation analysis between PSMA2 and *GLP-1R* expression in the T2D and non-T2D group separately. There was positive correlation in the T2D (r = 0.68, 95% CI: 0.02–0.92, P = 0.046, correlation test) but not in the non-T2D group (r = 0.29, 95% CI: 0.47–0.80, P = 0.46, correlation test) (Fig. 5e and f).

High glucose increased RNA and protein expression of GLP-1R in human and mouse cervical cancer cell lines (Fig. 5g–h, i–m). In CUP-1 cells, *GLP-1R* expression was increased in a glucose-dose-dependent manner (NG vs LG: ~3 folds, P = 0.001, *t-test*; HG vs NG: ~3 folds, P = 0.007, *t-test*) (Fig. 5h). Upon knockdown of *GLP-1R*, there was correspondingly reduced expression of *PSMA2* under normal and high glucose conditions (Fig. 5m–o).

5 High glucose activated NF-κB signalling pathway but attenuated by Exendin-4 in CUP-1 cells

We treated CUP-1 cells with or without Exendin-4 under normal or high glucose condition to evaluate the protein expression of *psma2* and NF-κB signalling inflammatory markers phospho-p65 and phospho-IκB. High glucose increased *psma2* protein expression (P = 0.02, *t-test*), which was attenuated by Exendin-4 (P = 0.003, *t-test*) (Fig. 6a and b). High glucose increased protein expression of phospho-p65 (P = 0.04, *t-test*) and phospho-IκB (P = 0.003, *t-test*), which were attenuated by Exendin-4 (Fig. 6c and d).

3. Discussion

In this translational study, we have used human and experimental studies to test the hypothesis regarding the roles of PSMA2 and GLP1-RA in cervical cancer with data summarised in Table 1. We discovered, PSMA2 and GLP-1R expression were increased and positively correlated in cervical cancer specimens from patients with T2D. Exendin-4 attenuated PSMA2 expression and tumour growth *in vivo* and *in vitro*. In TCGA database, *PSMA2* was over-expressed in 12 human cancer types. Experimentally, high glucose increased *PSMA2* expression in multiple human and mouse epithelial cervical cancer cell lines (CUP-1), the latter being glucose-dependent, but not in non-cancerous cells. In the CUP-1 cells, *psma2*-O/E and *psma2*-shRNA increased and decreased cell proliferation, respectively. *In vivo*, *psma2*-shRNA attenuated tumour growth and cell proliferation. *In vitro*, high glucose upregulated *psma2* expression and cell proliferation in CUP-1 cells, which were exacerbated with *psma2*-O/E but attenuated by Exendin-4. The latter also attenuated tumour growth, cell proliferation and PSMA2 expression *in vivo*. There was no difference in *GLP-1R* expression in 12 cancer types in TCGA database, albeit with unknown glycaemic status. *GLP-1R* expression was increased

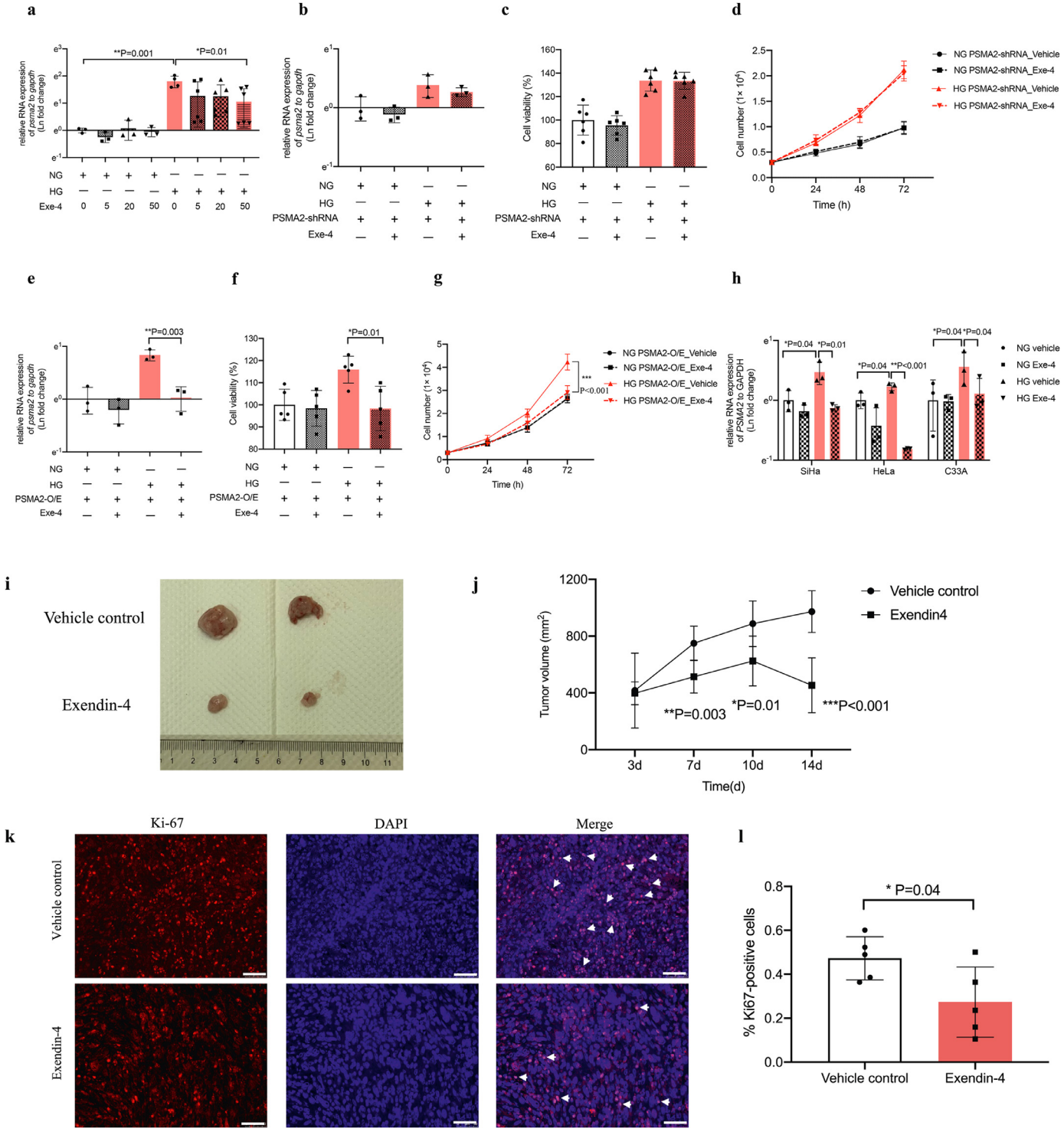

Fig. 4. Exendin-4 reduced PSMA2 expression, cell proliferation, and tumour volume *in vitro* and *in vivo*. (a) The RNA expression of *psma2* was measured in CUP-1 cells after treatment with Exendin-4 at the concentration of 0, 5, 20, and 50 nmol/L for 48 h in normal or high glucose medium. (b-d) The RNA expression of *psma2*, cell viability, and proliferation were examined in *psma2*-shRNA-CUP-1 cells with or without Exendin-4 treatment in normal or high glucose medium. (e-g) The RNA expression of *psma2*, cell viability, and proliferation were examined in *psma2*-O/E-CUP-1 cells with or without Exendin-4 treatment in normal or high glucose medium. (h) The RNA expression of *psma2* was examined in SiHa, HeLa, and C33A human cervical cancer cell lines with or without Exendin-4 treatment in normal or high glucose medium. (i-j) Tumour volume was measured twice weekly after inoculation of CUP-1 cells with treatment of Exendin-4 (30 nmol/kg) or vehicle (PBS) (N = 7 in each group). Cell proliferation marker Ki67 (k-l) (red: Ki67, blue: DAPI, magnification: × 200. The white scale bar represents 50 μm) and PSMA2 expression (m-n) were measured in the tumour of above diabetes/cancer mice (red: PSMA2, blue: DAPI, magnification: × 400. The white scale bar represents 25 μm). Data are presented as mean±SD with individual data points in histograms. * $p < 0.05$, ** $p < 0.01$, *** $p < 0.001$. (For interpretation of the references to color in this figure legend, reader can refer to the web version of this article.)

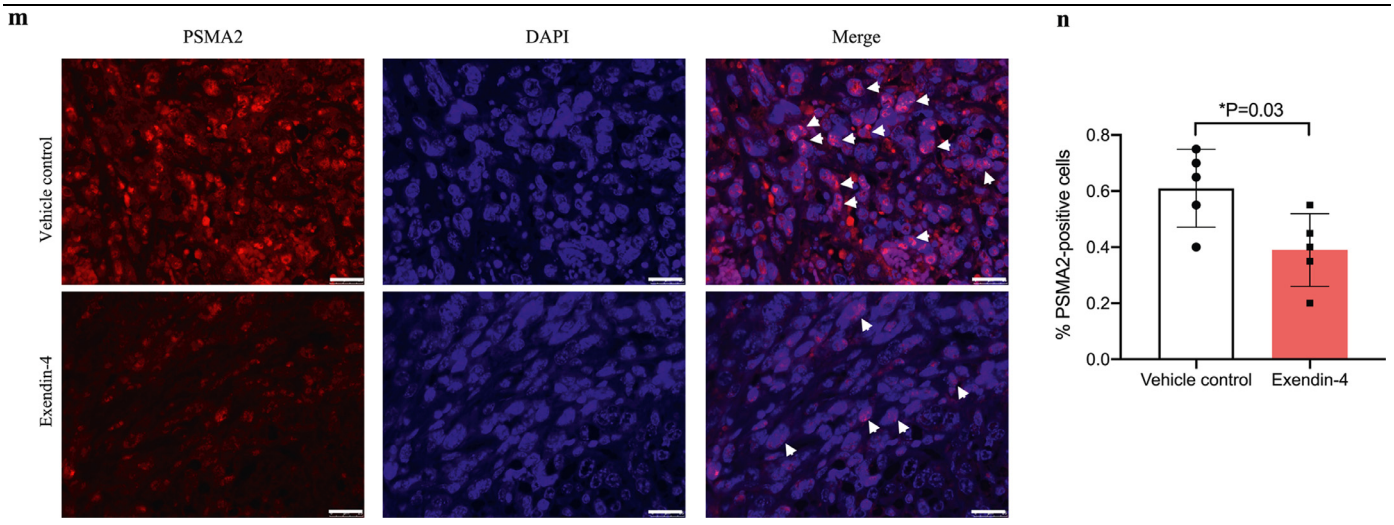

Fig. 4. Continued.

and positively correlated with *PSMA2* in cervical cancer specimens from patients with T2D, which were further validated by GLP-1R knockdown in CUP-1 cells. *GLP-1R* expression was increased in multiple human cervical cancer cell lines under high glucose condition and in CUP-1 cells in a glucose-dose-dependent manner. High glucose upregulated protein expression of *psma2*, p-P65, and p-IκB but attenuated by Exendin-4. Taken together, our data support the promoting effect of high glucose on *GLP-1R* and *PSMA2* expression in cervical cancer, which can be attenuated by Exendin-4.

In experimental studies of diabetes, high glucose impaired the ubiquitin-proteasome system function to cause abnormal cardiovascular-renal function and amyloid precipitation in islets [36]. High glucose activated the hexosamine-polyol-dicarbonyl methylglyoxial (MGO) pathways accompanied by decreased proteasome activity in diabetic kidney disease models [37]. On the other hand, MG132, a proteasome inhibitor, attenuated diabetic nephropathy by enhancing renal antioxidative capacity and histone degradation [38–40]. Increased proteasome expression was implicated in atherosclerosis [41], while insulin deficiency activated proteasome activity and caused cardiac muscle dysfunction [42]. However, these experimental results were not always consistent. In human studies, both decreased and increased proteasome expression had been reported in specimens from patients with T2D and cardiovascular disease [43]. In contrast, the upregulation of the ubiquitin-proteasome system had been consistently reported in carcinogenesis [44]. This was supported by the use of proteasome inhibitors as first-line adjunctive drugs in addition to conventional chemotherapy in patients with multiple myeloma to maximize efficacy and minimize treatment resistance [45].

Proteasome alpha subunit has seven isoforms encoded by seven genes *PSMA*1-7. In TCGA database, we noted increased *PSMA2* expression in 12 human cancer types, including cervical epithelial cancer. In vitro, we confirmed high glucose increased *PSMA2* expression and cell proliferation in cervical and breast cancer cell lines attenuated by Exendin-4 (SFig. 1). This effect was corroborated by increased tumour growth in the diabetes/cancer model. The proto-oncogenic role of *psma2* was confirmed by transfection studies where *psma2*-O/E enhanced, and *psma2*-shRNA reduced cancer growth. *In vivo, psma2*-shRNA did not alter blood glucose level, suggesting that this effect was independent of glucose-lowering effect (SFig. 2). These experimental results were corroborated by increased expression of *PSMA2* in cervical cancer specimens from patients with T2D. These original findings suggested that dysregulation of *PSMA2* might underlie the high risk of cancer in T2D. The glucose-dependent upregulation of *PSMA2* in breast cancer cells (SFig. 1a) and its increased expression in multiple cancer types in TCGA database, along with the genetic associations of *PSMA2* SNPs with various cancer types [14,15] suggest that the proto-oncogenic role of *PSMA2* might apply to other cancer cell types.

There are few studies which systemically examined the effects of hyperglycaemia on cancer and the therapeutic effects of glucose lowering drugs on cancer. The mechanism of Exendin-4 on tumour attenuation was multifactorial. Previous evidence indicated that Exendin-4 attenuated prostate tumour growth by inhibiting extracellular phosphorylation in signal-regulated kinase (ERK)-mitogen-activated protein kinase (MAPK) pathway and inhibition of NF-κB activation [23,46,47]. In our study, Exendin-4 reduced high-glucose-upregulated PSMA2 expression, but not in normal glucose condition in cervical cancer cells. Different cancer types might exhibit different behaviours with different dominant pathologies. Unlike prostate cancer, cervical cancer was mainly induced by HPV infection, and the inflammation might be exaggerated by hyperglycaemia [48]. The anti-inflammatory effect of Exendin-4 has been well reported [27,49]. PSMA was involved in proinflammatory pathways and whether the anti-cancer effect of Exendin-4 through PSMA reduction was mediated by anti-inflammation required further elucidation. Given the cross-talk between hyperglycaemia and inflammation [50], our study provided new insights regarding the potential of using Exendin-4 to treat cancer in patients with T2D.

The effect of hyperglycaemia on GLP-1R expression in cancer and non-cancer tissues might be different. Chronic hyperglycaemia decreased GLP-1R expression in pancreatic beta cells in diabetes, which might contribute towards the impaired incretin and insulin secretion [51]. In patients with obesity, decreased GLP-1R expression had been reported in vascular endothelial cells [52]. By contrast, increased expression of GLP-1R expression had been reported in various types of human tumour, including endocrine tumours and lung cancer [53,54]. According to the Warburg's hypothesis, cancer cells exhibit high rates of glycolysis with lactic acid production, which might require increased glucose uptake [55,56]. Taken together, we hypothesized that in cancer cells, hyperglycemia might increase GLP-1R expression to promote glucose uptake to fuel cell growth.

In support of this hypothesis, we demonstrated that high glucose increased GLP-1R expression in human and mouse epithelial cervical cancer cell lines. These findings were corroborated by increased expression of *PSMA2* and *GLP-1R* and their positive correlations in cervical cancer specimens only from patients with T2D. The cross-talk between *GLP-1R* and *PSMA2* pathways in carcinogenesis was

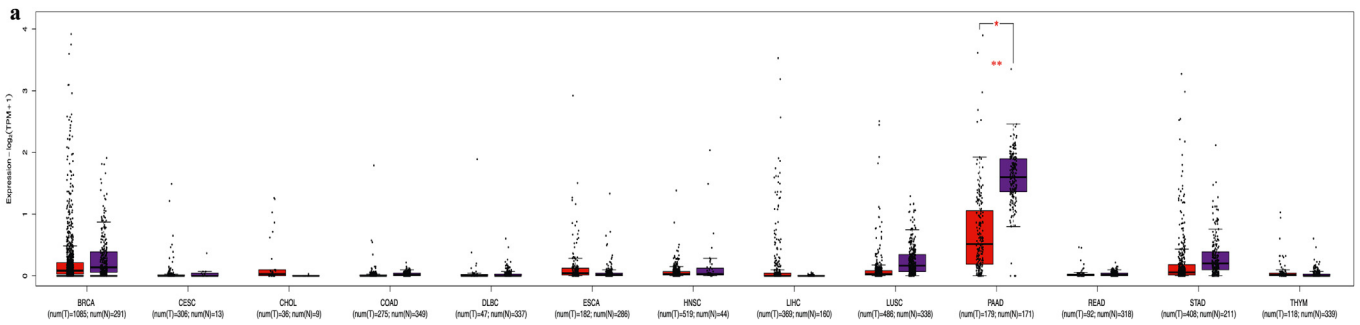

BRCA: Breast invasive carcinoma, CESC: Cervical squamous cell carcinoma and endocervical adenocarcinoma, CHOL: Cholangial carcinoma, COAD: Colon adenocarcinoma, DLBC: Lymphoid Neoplasm Diffuse Large B-cell Lymphoma, ESCA: Esophageal carcinoma, HNSC: Head and Neck squamous cell carcinoma, LIHC: Liver hepatocellular carcinoma, LUSC: Lung squamous cell carcinoma, PAAD: Pancreatic adenocarcinoma, READ: Rectum adenocarcinoma, STAD: Stomach adenocarcinoma, THYM: Thymoma
Red: cancer, purple: control ***P<0.001

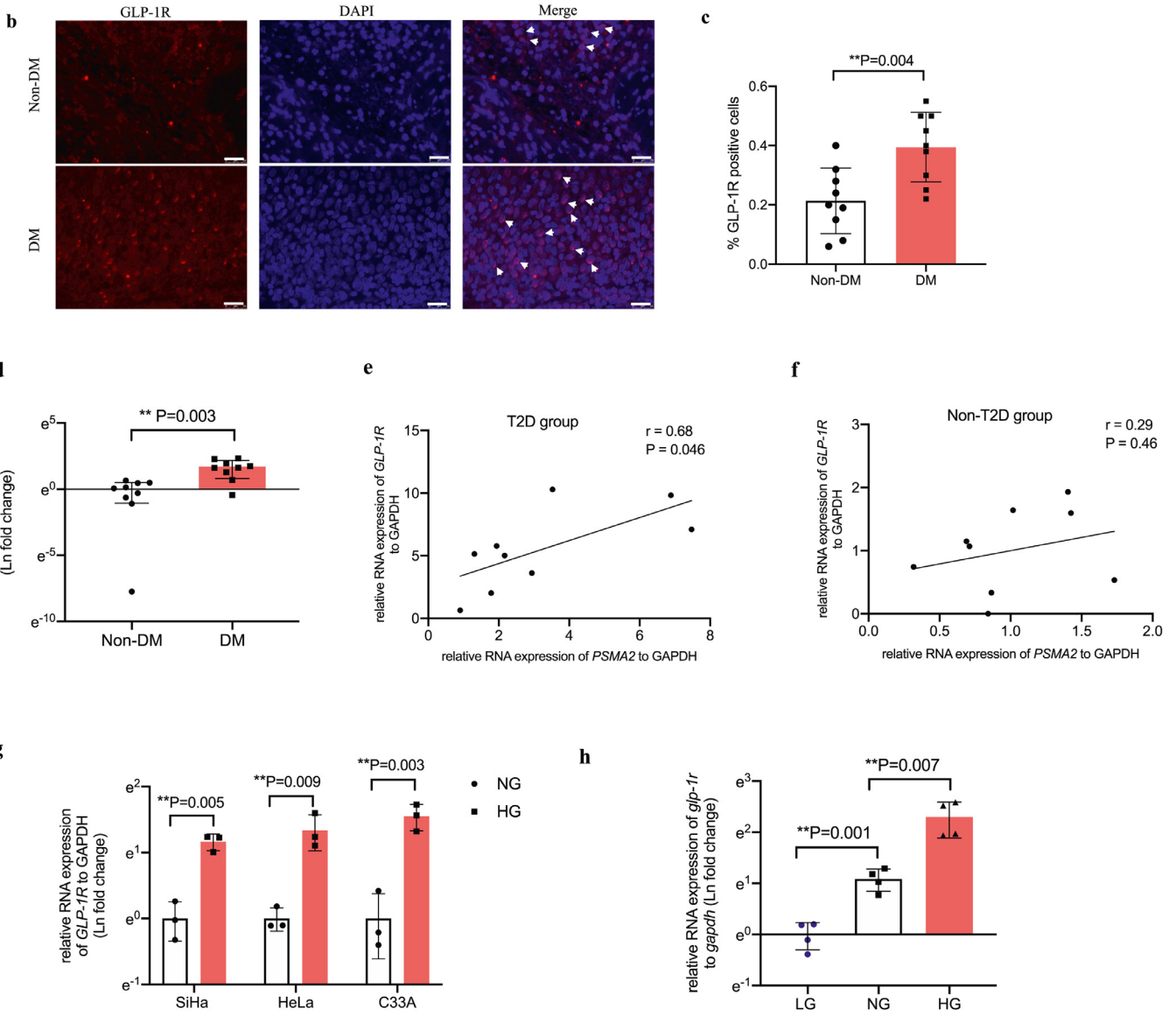

Fig. 5. In human cervical cancer specimen, GLP-1R expression was increased and positively correlated with *PSMA2* expression in patients with T2D, supplemented by experimental evidence in multiple cervical cancer systems. *GLP-1R* expression was examined in TCGA database (a). The protein (b, c) (red: GLP-1R, blue: DAPI, magnification: × 400. The white scale bar represents 25 μm) and RNA expression (d) of *GLP-1R* was examined in cervical cancer specimens from patients with and without T2D. (e-f) Correlation analysis was performed between *GLP-1R* and *PSMA2* expression in cervical cancer specimens from patients with and without T2D. The RNA expression of *GLP-1R* was examined in human cervical cancer cell lines (g) and CUP-1 cells (h). GLP-1R protein expression was examined in human cervical cancer cell lines under normal and high glucose medium (i-l). GLP-1R and PSMA2 protein expression in CUP-1 cells with or without GLP-1R siRNA transfection (m-o). Data are presented as mean±SD with individual data points in histograms. * $p < 0.05$, ** $p < 0.01$, *** $p < 0.001$. (For interpretation of the references to color in this figure legend, reader can refer to the web version of this article.)

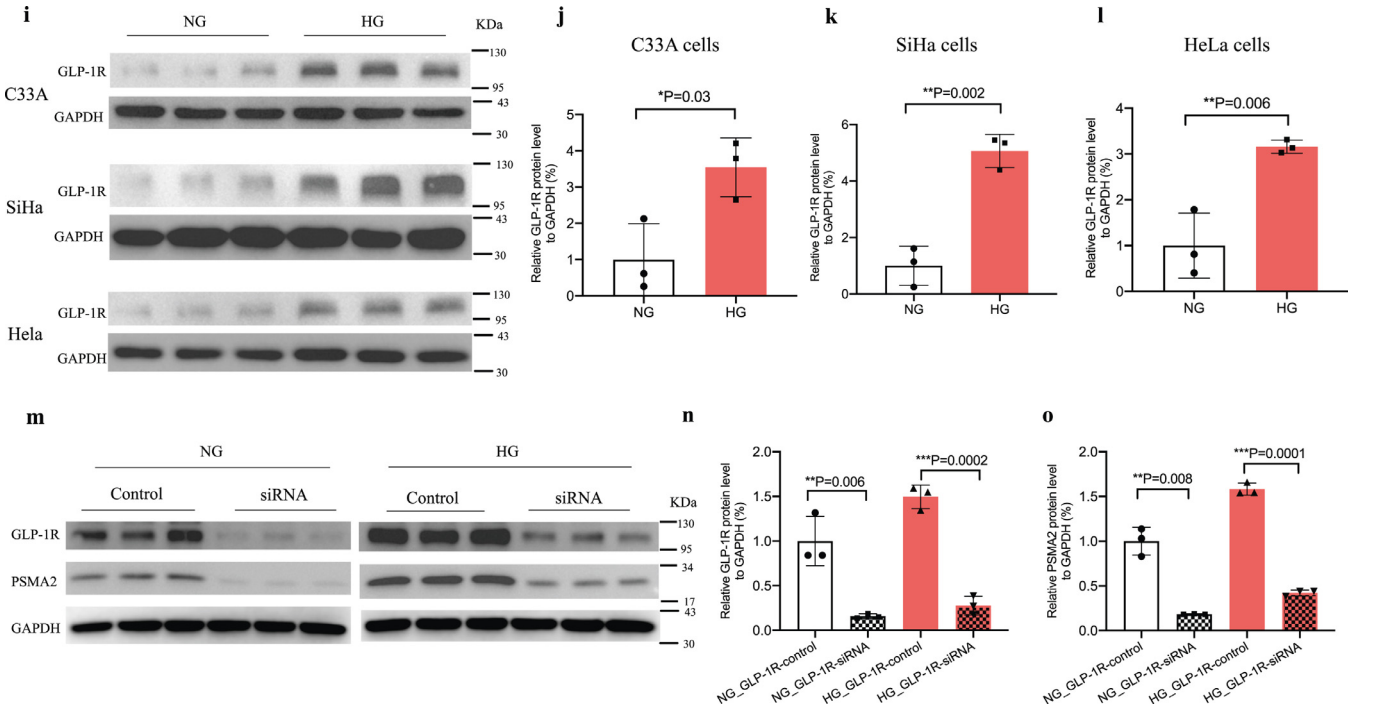

Fig. 5. Continued.

plausible. Proteasome inhibitor attenuated widespread inflammation by inhibiting the NF-κB pathway [57]. Proteasome could degrade IκB and liberated the inflammatory signal of P65 to activate subsequent nuclear transcription of inflammatory genes [58]. Other researchers had reported the anti-inflammatory effects of Exendin-4 on macrophage migration *in vitro* as well as on breast cancer growth [59,60]. In our study, Exendin-4 attenuated phosphorylation of the P65 and IκB in the NF-κB pathway, but the molecular mechanism underlying this inhibitory effect required further elucidation.

There are limitations in this study. More experiments are needed to elucidate the mechanism underlying the inhibitory effects of Exendin-4 on PSMA2 expression. The mechanisms underlying the activation of proteasome in cancer development is complex, including but not limited to chaperone protein overexpression, catalytic subunits downregulation, upstream enzymes and transcription factor activation [61]. The IKK inhibitor, a key blocker of the NF-κB pathway, can be used to determine whether the cancer-promoting effects of high glucose through *psma2* expression is mediated by the NF-κB pathway activation, which is known to promote inflammation and tumour growth [62]. We are currently designing a series of experiments to explore the molecular mechanisms underlying the cross-talk between PSMA2 and GLP-1R, which is beyond the scope of this

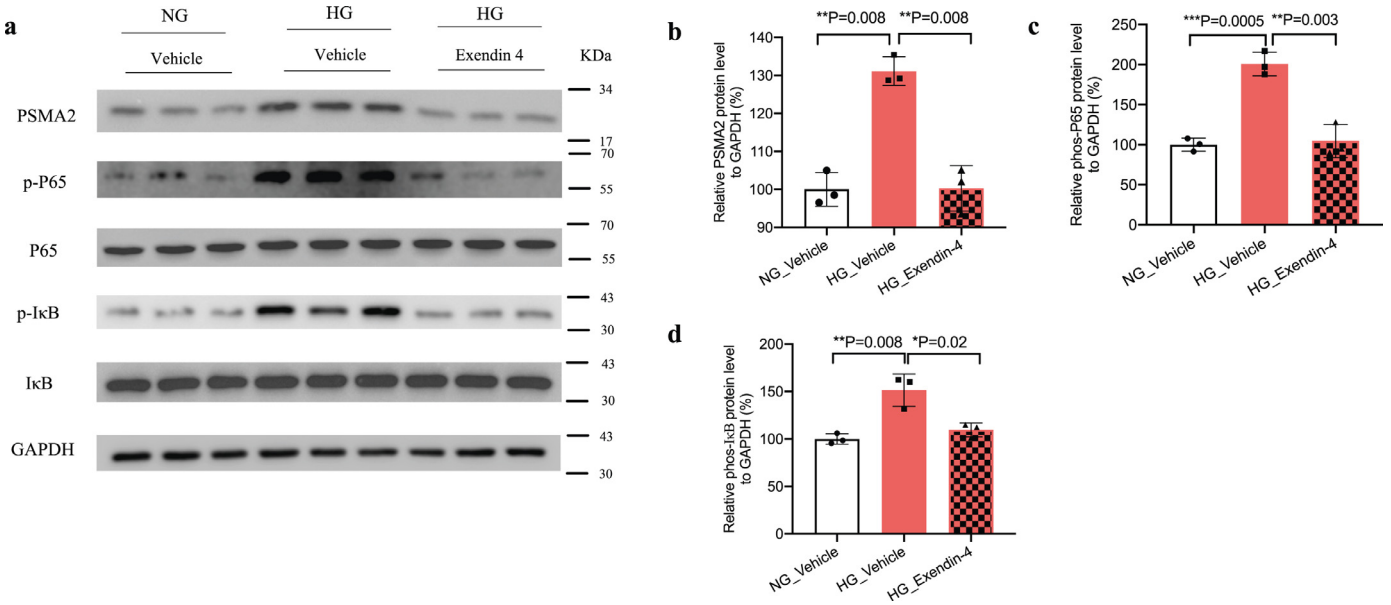

Fig. 6. High glucose activated NF-κB signalling pathway but attenuated by Exendin-4 in CUP-1 cells. (a-d) Quantitative data was calculated in each group. Data are presented as mean±SD with individual data points in histograms. * $p < 0.05$, ** $p < 0.01$, *** $p < 0.001$.

Table 1
Outcome measures in various experimental models.

Human cervical cancer		*Mouse epithelial cervical cancer (CUP-1)*	*Human cervical cancer cell lines (SiHa, Hela, C33A)*	*CUP-1-induced tumour model in db/db mice*	
1. TCGA database:		HG: ↑ PSMA2 RNA expression in a glucose-dose-dependent manner (Fig. 2f) HG: ↑ PSMA2 protein expression (Fig. 6a)	HG: ↑ PSMA2 RNA expression (Fig. 2e)		
1) ↑ PSMA2 RNA expression in 12 cancer types (Fig. 2a) *2)* (-) GLP-1R RNA expression in cancer (Fig. 5a)					
2. Human cervical cancer samples from PWH-CUHK:		HG: ↑ cell viability and proliferation (Fig. 3a, b) PSMA2-O/E: ↑ cell viability and proliferation (Fig. 3a, b) PSMA2-shRNA: ↓ cell viability and proliferation (Fig. 3c, d) PSMA2-O/E and PSMA2-shRNA validation (Fig. 3e-h)		*1.* PSMA2-shRNA: ↓ tumour volume (Fig. 3i-j)	
1) ↑ PSMA2 protein expression in T2D (Fig. 1b, c)					
Non-T2D: 0.36% (0.25-0.46)	T2D: 0.59% (0.47-0.72)			*2.* PSMA2-shRNA: ↓ Ki67 protein expression in tumour (Fig. 3k, l)	
2) ↑ PSMA2 RNA expression in T2D (Fig. 2d)				Vector control: 0.46% (0.32- 0.60)	PSMA2-shRNA vehicle: 0.26% (0.09-0.42)
Non-T2D: 1.00 (0.66-1.34)	T2D: 3.22 (1.38-5.05) (fold change)	Exe-4: ↓ PSMA2 RNA (Fig. 4a) and protein (Fig. 6a) expression under HG Exe-4: ↓ PSMA2 RNA expression, ↓ cell viability and proliferation under HG in PSMA2-O/E cells (Fig. 4e-g) Exe-4: (-) PSMA2 RNA expression, (-) cell viability and proliferation in PSMA2-shRNA cells (Fig. 4b-d)	Exe-4: ↓ PSMA2 RNA expression under HG (Fig. 4h)	*3.* Exe-4: ↓ tumour volume (Fig. 4i, j)	
3) ↑ GLP-1R protein expression in T2D (Fig. 5b, c)				*4.* Exe-4: ↓ Ki67 protein expression in tumour (Fig. 4k, l)	
Non-T2D: 0.21% (0.13-0.30)	T2D: 0.39% (0.30-0.48)	HG: ↑ GLP-1R RNA expression in a glucose-dose-dependent manner (Fig. 5h) HG: ↑ GLP-1R protein expression (Fig. 5i) GLP-1R siRNA: ↓ PSMA2 protein expression in (Fig. 5m-o) HG: ↑ p-P65, p-IκB protein expression, but ↓ by Exe-4 (Fig. 6a-d)	HG: ↑ GLP-1R RNA and protein expression (Fig. 5g, i-l)	Vehicle control: 0.47% (0.35-0.59)	Exe-4: 0.27% (0.07- 0.47)
4) ↑ GLP-1R RNA expression in T2D (Fig. 5d)				*5.* Exe-4: ↓ PSMA2 protein expression in tumour (Fig. 4m, n)	
Non-T2D: 1.00 (0.5-1.5)	T2D: 5.49 (3.00-7.98) (fold change)				
5) (+) correlation in RNA expression between PSMA2 and GLP-1R in T2D, but not in non-T2D. (Fig. 5e, f)				Vehicle control: 0.61% (0.44-0.78)	Exe-4: 0.39% (0.23-0.55)
Non-T2D: r= 0.29 (0.47-0.80)	T2D: r=0.68 (0.02-0.92)				

↑: increase; ↓: decrease; (-): no change; T2D: type 2 diabetes; Exe-4: exendin-4; TCGA: the Cancer Genome Atlas Program; HG: high glucose; O/E: overexpression. Data are presented as point estimate and 95% confidence interval (CI).

Table 2
Clinical characteristics of patients with cervical cancer selected for analysis.

Case No.	Age (Y)	Ethnicity	Date of Operation (dd/mm/year)	T2D	HbA1c (%)
C1208	58	Chinese	22/12/2017	Yes	11.9
C1191	84	Chinese	04/08/2017	Yes	6.8
C1180	57	Chinese	19/04/2017	Yes	7.6
C1083	50	Chinese	15/09/2014	Yes	6.5
C1177	57	Chinese	19/04/2017	Yes	7.6
C1137	41	Chinese	18/01/2016	Yes	7.5
C1213	40	Chinese	18/01/2019	Yes	6.9
C1234	54	Chinese	29/04/2019	Yes	9.4
C1219	51	Chinese	09/02/2018	Yes	Nil*
C1195	84	Chinese	17/08/2017	No	5.5
C1203	37	Chinese	22/11/2017	No	5.1
C1210	51	Chinese	05/01/2018	No	Nil
C1220	59	Chinese	22/03/2018	No	Nil
C1228	61	Chinese	18/05/2018	No	Nil
C1229	56	Chinese	08/06/2018	No	Nil
C1157	47	Chinese	22/08/2016	No	Nil
C1185	70	Chinese	17/05/2017	No	Nil
C1182	38	Chinese	24/04/2017	No	Nil

*documented physician-diagnosed T2D.

paper. In our *in vivo* studies, we had only measured tumour volume. Although it is preferable to measure both tumour weight and tumour volume, the latter had been reported as the only measurement by other workers [63]. The case-control clinical study was subject to selection bias since only samples from Chinese women were included. We did not adjust for confounding factors such as treatment or other risk factors. Further studies in other ethnic groups will be required to validate these observations. However, the increased expression of PSMA2 and GLP-1R and their positive correlation in patients with T2D concorded with the results from our experimental studies.

In sum, our consistent results allow us to conclude that high glucose increased *PSMA2* expression and promoted tumour growth, which could be attenuated by Exendin-4. The latter effects might be mediated by reducing *psma2* and NF-κB pathway activity. Since proteasome inhibitors and GLP-1 mimetics are in clinical use, our data have strong translational potential, especially in patients with T2D and cancer, which co-expressed *PSMA2* and *GLP-1R*. In these patients, the anti-cancer effect of Exendin-4 should be explored in clinical trials.

Contributors

Principal design of the study, conception of study, writing of manuscript: J.C, D.M, V.W.Y.L, Design of experiments and interpretation of data: D.M, J.C., P.K.S.C, Histopathological analysis and interpretation: D.M, H.C., Human sample process: D.M, C.C.W, J.K, J.J.X., Bioinformatic analysis: M.S., Experimental procedures: D.M, X. M, H.M.L, X.Y.T, C.K.W, E.C, A.P.S.K., Data verification: D.M and Y.H.

All authors have read and approved the final version of the manuscript with access to the raw data.

Data sharing statement

All datasets generated or analysed in the current study are available from the corresponding author on reasonable request.

Declaration of Competing Interest

JCNC reported receiving research grants and/or honoraria for consultancy or giving lectures from AstraZeneca, Boehringer Ingelheim, Eli Lilly, Merck Serono, Merck Sharp & Dohme, Pfizer, and Sanofi. EC reported receiving grants from Lee Powder and Sanofi. VWYL received a University-Industry Collaboration Program (UIM/329; from the Innovation and Technology Fund, Hong Kong government, and Lee's Pharmaceutical [Hong Kong Limited] in 2018–2020) and served as a scientific consultant for Novartis Pharmaceutical (Hong Kong) Limited (Oct 2015–Oct 2016).

Acknowledgements

This project was supported by the CUHK Postdoctoral Fellowship Scheme. CUHK Direct Grant and CUHK Diabetes Research and Education Fund of the Department of Medicine and Therapeutics, Faculty of Medicine, CUHK.

VWYL is funded by the General Research Fund (#17121616, #14168517), Research Impact Fund (#R4017-18) from Research Grant Council, Hong Kong; the Health and Medical Research Fund (HMRF #15160691, the Health and Medical Research Fund, the Food and Health Bureau, the Government of the Hong Kong SAR), University-Industry Collaboration Program (UIM/329; Innovation and Technology Fund, Hong Kong government), and the Hong Kong Cancer Fund.

Supplementary materials

Supplementary material associated with this article can be found, in the online version, at doi:10.1016/j.ebiom.2021.103242.

References

[1] Rao Kondapally Seshasai S, Kaptoge S, Thompson A, Di Angelantonio E, Gao P, Sarwar N, et al. Diabetes mellitus, fasting glucose, and risk of cause-specific death. N Engl J Med 2011;364(9):829–41.
[2] Yang X, Lee HM, Chan JC. Drug-subphenotype interactions for cancer in type 2 diabetes mellitus. Nat Rev Endocrinol 2015;11(6):372–9.
[3] Yang X, Ko GT, So WY, Ma RC, Yu LW, Kong AP, et al. Associations of hyperglycemia and insulin usage with the risk of cancer in type 2 diabetes: the Hong Kong diabetes registry. Diabetes 2010;59(5):1254–60.
[4] zur Hausen H. Papillomaviruses and cancer: from basic studies to clinical application. Nat Rev Cancer 2002;2(5):342–50.
[5] Coussens LM, Werb Z. Inflammation and cancer. Nature 2002;420(6917):860–7.
[6] Chen S, Tao M, Zhao L, Zhang X. The association between diabetes/hyperglycemia and the prognosis of cervical cancer patients: a systematic review and meta-analysis. Medicine 2017;96(40):157–65.
[7] Crawford LJ, Walker B, Irvine AE. Proteasome inhibitors in cancer therapy. J Cell Commun Signal 2011;5(2):101–10.
[8] Meng X, Zhong J, Liu S, Murray M, Gonzalez-Angulo AM. A new hypothesis for the cancer mechanism. Cancer Metastasis Rev 2012;31(1-2):247–68.
[9] Jang HH. Regulation of protein degradation by proteasomes in cancer. J Cancer Prev 2018;23(4):153–61.
[10] Adams J. The proteasome: structure, function, and role in the cell. Cancer Treat Rev 2003;29:3–9.
[11] Arlt A, Bauer I, Schafmayer C, Tepel J, Müerköster SS, Brosch M, et al. Increased proteasome subunit protein expression and proteasome activity in colon cancer relate to an enhanced activation of nuclear factor E2-related factor 2 (Nrf2). Oncogene 2009;28(45):3983–96.
[12] Hideshima T, Richardson P, Chauhan D, Palombella VJ, Elliott PJ, Adams J, et al. The proteasome inhibitor PS-341 inhibits growth, induces apoptosis, and overcomes drug resistance in human multiple myeloma cells. Cancer Res 2001;61(7):3071–6.
[13] Petrocca F, Altschuler G, Tan SM, Mendillo ML, Yan H, Jerry DJ, et al. A genome-wide siRNA screen identifies proteasome addiction as a vulnerability of basal-like triple-negative breast cancer cells. Cancer Cell 2013;24(2):182–96.
[14] Sjöblom T, Jones S, Wood LD, Parsons DW, Lin J, Barber TD, et al. The consensus coding sequences of human breast and colorectal cancers. Science 2006;314(5797):268–74.
[15] Gomes AV. Genetics of proteasome diseases. Scientifica 2013;2013:629–49.
[16] Moreau P, Richardson PG, Cavo M, Orlowski RZ, San Miguel JF, Palumbo A, et al. Proteasome inhibitors in multiple myeloma: 10 years later. Blood 2012;120(5):947–59.
[17] Kim W, Egan JM. The role of incretins in glucose homeostasis and diabetes treatment. Pharmacol Rev 2008;60(4):470–512.
[18] Shyangdan DS, Royle P, Clar C, Sharma P, Waugh N, Snaith A. Glucagon-like peptide analogues for type 2 diabetes mellitus. Cochrane Database Syst Rev 2011;2011(10):276–8.
[19] Dicker D. DPP-4 Inhibitors. Impact on glycemic control and cardiovascular risk factors. 2011;34:276-8.
[20] Nomiyama T, Kawanami T, Irie S, Hamaguchi Y, Terawaki Y, Murase K, et al. Exendin-4, a GLP-1 receptor agonist, attenuates prostate cancer growth. Diabetes 2014;63(11):3891–905.

[21] Wenjing H, Shao Y, Yu Y, Huang W, Feng G, Li J. Exendin-4 enhances the sensitivity of prostate cancer to enzalutamide by targeting Akt activation. Prostate 2020;80(5):367–75.
[22] Zhao HJ, Jiang X, Hu LJ, Yang L, Deng LD, Wang YP, et al. Activation of GLP-1 receptor enhances the chemosensitivity of pancreatic cancer cells. J Mol Endocrinol 2020;64(2):103–13.
[23] Iwaya C, Nomiyama T, Komatsu S, Kawanami T, Tsutsumi Y, Hamaguchi Y, et al. Exendin-4, a glucagonlike peptide-1 receptor agonist, attenuates breast cancer growth by inhibiting NF-κB activation. Endocrinology 2017;158(12):4218–32.
[24] Cao C, Yang S, Zhou Z. GLP-1 receptor agonists and risk of cancer in type 2 diabetes: an updated meta-analysis of randomized controlled trials. Endocrine 2019;66(2):157–65.
[25] Nomiyama T, Yanase T. GLP-1 receptor agonist as treatment for cancer as well as diabetes: beyond blood glucose control. Expert Rev Endocrinol Metab 2016;11(4):357–64.
[26] Insuela DBR, Carvalho VF. Glucagon and glucagon-like peptide-1 as novel anti-inflammatory and immunomodulatory compounds. Eur J Pharmacol 2017;812:64–72.
[27] He L, Wong CK, Cheung KK, Yau HC, Fu A, Zhao HL, et al. Anti-inflammatory effects of exendin-4, a glucagon-like peptide-1 analog, on human peripheral lymphocytes in patients with type 2 diabetes. J Diabetes Investig 2013;4(4):382–92.
[28] Kong AP, Chan JC. Cancer risk in type 2 diabetes. Curr Diab Rep 2012;12(4):325–8.
[29] Kong AP, Yang X, So WY, Luk A, Ma RC, Ozaki R, et al. Additive effects of blood glucose lowering drugs, statins and renin-angiotensin system blockers on all-site cancer risk in patients with type 2 diabetes. BMC Med 2014;12:76–86.
[30] He L, Law PT, Boon SS, Zhang C, Ho WC, Banks L, et al. Increased growth of a newly established mouse epithelial cell line transformed with HPV-16 E7 in diabetic mice. PLoS One 2016;11(10):1–11.
[31] He L, Law PTY, Wong CK, Chan JCN, Chan PKS. Exendin-4 exhibits enhanced antitumor effects in diabetic mice. Sci Rep 2017;7(1):1791–801.
[32] Tomczak K, Czerwińska P, Wiznerowicz M. The Cancer Genome Atlas (TCGA): an immeasurable source of knowledge. Contemp Oncol 2015;19(1A):A68–77.
[33] Tang Z, Kang B, Li C, Chen T, Zhang Z. GEPIA2: an enhanced web server for large-scale expression profiling and interactive analysis. Nucleic Acids Res 2019;47(W1):556–60.
[34] Lonsdale J, Thomas J, Salvatore M, Phillips R, Lo E, Shad S, et al. The Genotype-Tissue Expression (GTEx) project. Nat Genet 2013;45(6):580–5.
[35] Wolf I, O'Kelly J, Rubinek T, Tong M, Nguyen A, Lin BT, et al. 15-hydroxyprostaglandin dehydrogenase is a tumor suppressor of human breast cancer. Cancer Res 2006;66(15):7818–23.
[36] Aghdam SY, Gurel Z, Ghaffarieh A, Sorenson CM, Sheibani N. High glucose and diabetes modulate cellular proteasome function: implications in the pathogenesis of diabetes complications. Biochem Biophys Res Commun 2013;432(2):339–44.
[37] Queisser MA, Yao D, Geisler S, Hammes HP, Lochnit G, Schleicher ED, et al. Hyperglycemia impairs proteasome function by methylglyoxal. Diabetes 2010;59(3):670–8.
[38] Luo ZF, Qi W, Feng B, Mu J, Zeng W, Guo YH, et al. Prevention of diabetic nephropathy in rats through enhanced renal antioxidative capacity by inhibition of the proteasome. Life Sci 2011;88(11–12):512–20.
[39] Huang W, Yang C, Nan Q, Gao C, Feng H, Gou F, et al. The proteasome inhibitor, MG132, attenuates diabetic nephropathy by inhibiting SnoN degradation in vivo and in vitro. BioMed Res Int 2014:684765.
[40] Gao C, Chen G, Liu L, Li X, He J, Jiang L, et al. Impact of high glucose and proteasome inhibitor MG132 on histone H2A and H2B ubiquitination in rat glomerular mesangial cells. J Diabetes Res 2013:589474.
[41] Marfella R, DA M, Di Filippo C, Siniscalchi M, Sasso FC, Ferraraccio F, et al. The possible role of the ubiquitin proteasome system in the development of atherosclerosis in diabetes. Cardiovasc Diabetol 2007;6:35–46.
[42] Hu J, Klein JD, Du J, Wang XH. Cardiac muscle protein catabolism in diabetes mellitus: activation of the ubiquitin-proteasome system by insulin deficiency. Endocrinology 2008;149(11):5384–90.
[43] Liu H, Yu S, Xu W, Xu J. Enhancement of 26S proteasome functionality connects oxidative stress and vascular endothelial inflammatory response in diabetes mellitus. Arterioscler Thromb Vasc Biol 2012;32(9):2131–40.
[44] Adams J. The development of proteasome inhibitors as anticancer drugs. Cancer Cell 2004;5(5):417–21.
[45] Richardson PG, Weller E, Lonial S, Jakubowiak AJ, Jagannath S, Raje NS, et al. Lenalidomide, bortezomib, and dexamethasone combination therapy in patients with newly diagnosed multiple myeloma. Blood 2010;116(5):679–86.
[46] Kawamami T, Nomiyama T, Hamaguchi Y, Tanaka T, Yanase T. Exendin-4, a glucagon-like peptide-1 receptor agonist, attenuates prostate cancer cell proliferation via phosphorylation of MKP-1. Diabetes 2018;67:1957–68.
[47] Nie ZJ, Zhang YG, Chang YH, Li QY, Zhang YL. Exendin-4 inhibits glioma cell migration, invasion and epithelial-to-mesenchymal transition through GLP-1R/sirt3 pathway. Biomed Pharmacother 2018;106:1364–9.
[48] Tsalamandris S, Antonopoulos AS, Oikonomou E, Papamikroulis G-A, Vogiatzi G, Papaioannou S, et al. The role of inflammation in diabetes: current concepts and future perspectives. Eur Cardiol 2019;14(1):50–9.
[49] Pastel E, Joshi S, Knight B, Liversedge N, Ward R, Kos K. Effects of Exendin-4 on human adipose tissue inflammation and ECM remodelling. Nutr Diabetes 2016;6(12):1–10.
[50] Chang SC, Yang WV. Hyperglycemia, tumorigenesis, and chronic inflammation. Crit Rev Oncol Hematol 2016;108:146–53.
[51] Xu G, Kaneto H, Laybutt DR, Duvivier-Kali VF, Trivedi N, Suzuma K, et al. Downregulation of GLP-1 and GIP receptor expression by hyperglycemia: possible contribution to impaired incretin effects in diabetes. Diabetes 2007;56(6):1551–8.
[52] Kimura T, Obata A, Shimoda M, Shimizu I, da Silva, Xavier G, Okauchi S, et al. Down-regulation of vascular GLP-1 receptor expression in human subjects with obesity. Sci Rep 2018;8(1):10644.
[53] Körner M, Stöckli M, Waser B, Reubi JC. GLP-1 receptor expression in human tumors and human normal tissues: potential for in vivo targeting. J Nucl Med 2007;48(5):736–43.
[54] Körner M, Christ E, Wild D, Reubi JC. Glucagon-like peptide-1 receptor overexpression in cancer and its impact on clinical applications. Front Endocrinol 2012;3:158.
[55] Warburg O. On the origin of cancer cells. Science 1956;123(3191):309–14.
[56] DeBerardinis RJ, Chandel NS. We need to talk about the Warburg effect. Nat Metab 2020;2(2):127–9.
[57] Cullen SJ, Ponnappan S, Ponnappan U. Proteasome inhibition up-regulates inflammatory gene transcription induced by an atypical pathway of NF-kappaB activation. Biochem Pharmacol 2010;79(5):706–14.
[58] Liu T, Zhang L, Joo D, Sun S-C. NF-κB signaling in inflammation. Signal Transduct Targeted Ther 2017;2(1):17023–30.
[59] Ma GF, Chen S, Yin L, Gao XD, Yao WB. Exendin-4 ameliorates oxidized-LDL-induced inhibition of macrophage migration in vitro via the NF-κB pathway. Acta Pharmacol Sin 2014;35(2):195–202.
[60] Iwaya C, Nomiyama T, Komatsu S, Kawanami T, Tsutsumi Y, Hamaguchi Y, et al. Exendin-4, a glucagon like peptide-1 receptor agonist, attenuates breast cancer growth by inhibiting NF-κB activation. Endocrinology 2017;158(12):4218–32.
[61] Chondrogianni N, Voutetakis K, Kapetanou M, Delitsikou V, Papaevgeniou N, Sakellari M, et al. Proteasome activation: an innovative promising approach for delaying aging and retarding age-related diseases. Ageing Res Rev 2015;23:37–55.
[62] Taniguchi K, Karin M. NF-κB, inflammation, immunity and cancer: coming of age. Nat Rev Immunol 2018;18(5):309–24.
[63] Zhang K, Loong SL, Connor S, Yu SW, Tan SY, Ng RT, et al. Complete tumor response following intratumoral 32P BioSilicon on human hepatocellular and pancreatic carcinoma xenografts in nude mice. Clin Cancer Res 2005;11(20):7532–7.